Ab initio transmission electron microscopy image simulations of coherent Ag-MgO interfaces

S. Mogck, B. J. Kooi, and J. Th. M. De Hosson*
Department of Applied Physics, Materials Science Centre and Netherlands Institute of Metals Research, University of Groningen, Nijenborgh 4, 9747 AG Groningen, The Netherlands

M. W. Finnis
Atomistic Simulation Centre, School of Mathematics and Physics, Queen's University of Belfast, BT7 1NN Belfast, Northern Ireland
(Received 16 June 2004; revised manuscript received 21 September 2004; published 23 December 2004)

Density-functional theory calculations, within the plane-wave-ultrasoft pseudopotential framework, were performed in the ⟨110⟩ projection for MgO and for the coherent {111} Ag-MgO polar interface. First-principles calculations were incorporated in high-resolution transmission electron microscopy (HRTEM) simulations by converting the charge density into electron scattering factors to examine the influence of charge transfer, charge redistribution at the interface, and ionicity on the dynamical electron scattering and on calculated HRTEM images. It is concluded that the ionicity of oxides and the charge redistribution at interfaces play a significant role in HRTEM image simulations. In particular, the calculations show that at oxygen-terminated {111} Ag—MgO interfaces the first oxygen layer at the interface is much brighter than that in calculations with neutral atoms, in agreement with experimental observations.

DOI: 10.1103/PhysRevB.70.245427 PACS number(s): 68.35.Md, 68.37.−d, 61.72.Ff, 87.64.Ee

I. INTRODUCTION

Metal ceramic interfaces play an important role in the performance of many advanced materials[1–3] Examination of the atomistic structure with high-resolution transmission electron microscopy (HRTEM) may lead to a more fundamental insight into the adhesion and the nature of bonding between dissimilar materials.[1] In fact, the heterophase interface structure is a fingerprint of possible bonding across the interface. Interface dislocations serve as detectors of the coupling between these dissimilar materials and HRTEM serves as a sensor.[1] Nevertheless, to determine the atomic structure of interfaces it is essential that experimental HRTEM observations are compared with image simulations. Quantitative structure retrieval from HRTEM micrographs has demonstrated the need of incorporating atomic bonding, i.e., a more accurate description of the electron scattering in thin crystals.[4,5] At present HRTEM image simulations rely on scattering factors of neutral atoms and standard calculation of dynamic electron diffraction starts with a superposition of the scattering potential of atoms. The atomic form factors are presented in the literature,[6] but only at specific sampling points. To interpolate the atomic form factors for any spatial frequency the data are fitted using a sum of Gaussian functions as introduced by Doyle and Turner.[6] However, the difference between neutral and ionic scattering is very significant.[7] On the other hand, detailed experimental investigations on structure factors obtained with the convergent beam electron diffraction technique[8] revealed that the effect of ionicity on images is rather small. Furthermore, the effect of ionicity on HRTEM image simulations based on first-principles calculations was studied in sapphire by Gemming *et al.*,[9] who found no significant difference with simulated images of neutral atoms. On the other hand, Fresnel-like features are expected to be present at places where the mean inner potential changes rapidly[10,11] and this observation is relevant for metal-oxide interfaces.

This paper concentrates on the effect of charge redistribution and charge transfer at polar Ag-MgO interfaces, at which we expect electron transfer from the terminating Ag atoms to the terminating oxygens. This serves as an ideal model system, since its electronic structure and energy can be calculated reliably within the framework of density-functional theory (DFT). We expect that the qualitative effects of this charge transfer on HTREM images will be generalized to other cases of polar-oxide–metal interfaces The meaning here of *polar*, we recall, is that the oxide surface itself would be nonstoichiometric, carrying an excess of charge, if constructed without the metal to which it is bonded. If the metal to which it is bonded is also a component of the oxide, then of course no unambiguous separation of metal and oxide can be made.

For a comparison with experimental observations reference is made to Refs. 1 and 12–14. Metal-oxide interfaces were fabricated by internal oxidation to obtain many small oxide precipitates inside a metal matrix. This method produces many clean interfaces for investigations in each sample and such internally oxidized samples are easy to prepare for transmission electron microscopy. MgO precipitates in Ag after internal oxidation show no clear facets and are nearly spherical with a size of 5 nm.[12] A more complex system, for which no first-principles calculations have yet been made, is obtained by internal oxidation of Ag−3 at. % Mn at 900 °C for 1 h. The product in this case comprises Mn_3O_4 (tetragonal distorted spinel, $I4/amd$) precipitates bound by {111} planes with a size of 5–20 nm.[13] Figure 1 shows an example of a HRTEM image of in the ⟨110⟩ viewing direction of a polar {111} Ag—Mn_3O_4 interface. At the interface a distinct bright line, as indicated by the arrow, is present that can be a consequence of the bonding, image charge formation in the metal as a reaction to the polar interface and/or charge transfer. In order to test if these effects significantly influence HRTEM images, image simulations of the Ag-MgO interface based on the charge-density distribution

 ©2004 The American Physical Society

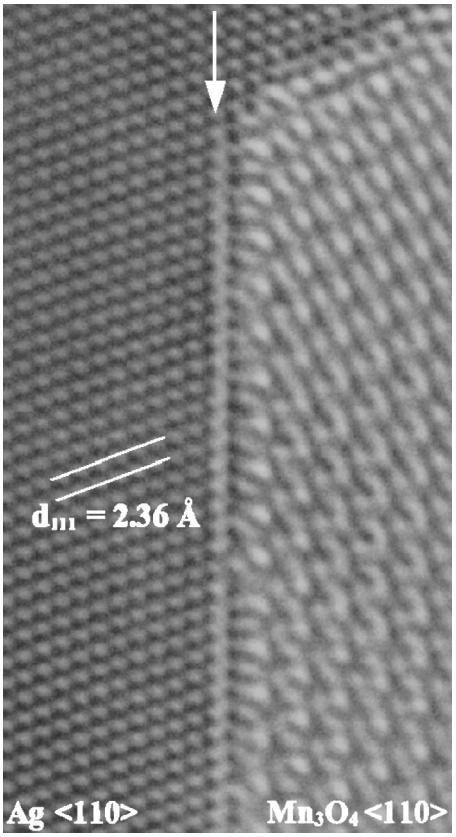

FIG. 1. Experimental HRTEM micrograph of an {111} Ag - Mn_3O_4 interface in the ⟨110⟩ viewing direction. The bright line at the outermost monolayer at the metal side of the interface is indicated by a white arrow.

derived form first-principles calculations are performed. The bonding across the interface is analyzed by comparing the "realistic" interface calculations with those involving atomic blocks with free surfaces and with those of neutral atoms. In this way, our study addresses the question if the "realistic" image simulations of HRTEM images lead to deviations (at the interface only or at both the interface and within the bulk) from the simulation involving only neutral atoms.

II. CHARGE-DENSITY CALCULATIONS

First-principles calculations were performed to calculate the charge distribution $\rho(\vec{r})$ of {111} Ag—MgO interfaces. This was carried out using the software packages CASTEP (Ref. 15) and DACAPO (developed at CAMP, Lyngby, Denmark[16]). CASTEP and DACAPO allow us to find the total energy, electron charge density, and electronic structure of a system of electrons and classical nuclei in their ground state, using ultrasoft pseudopotentials[17] and a basis of plane waves. In all our calculations, the cutoff energy of the plane-wave basis set of 340 eV was taken. DFT within the local-density approximation (LDA) with the Perdew-Zunger exchange-correlation functional[18] was applied in CASTEP and the Perdew-Wang generalized gradient approximation (GGA)[19] was applied in DACAPO. This is in accordance with the generated Vanderbilt ultrasoft pseudopotentials in both DFT codes. GGA calculations using pseudopotentials derived within LDA can differ significantly from those using pseudopotentials generated in GGA mode.[20] It is therefore advisable, for reasons of consistency, to use the same exchange-correlation functional for the applications as was used to generate the component pseudopotentials.

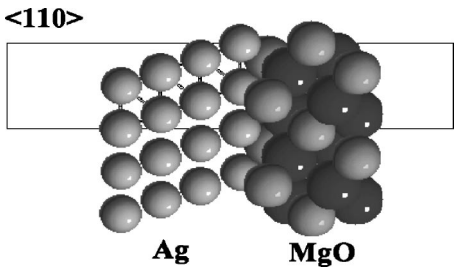

FIG. 2. Schematic illustration of the {111} Ag-MgO model with vacuum on both sides of the interface. This model is used to obtain the relaxed Ag coordinates for a model without the presence of a vacuum (see Fig. 3).

The {111} Ag-MgO interface is known to be semicoherent with a mismatch of 3.07%. The ratio of the MgO and Ag lattice constants is approximately 34/33 and with this ratio, the smallest possible periodic structure representing the interface would contain at least 999 Mg or O atoms and 1156 Ag atoms, which is currently far too big for first-principles calculations. Nevertheless, this small mismatch implies that a substantial fraction of the interface is coherent. Calculations on the {111} coherent Ag-MgO interface therefore provide realistic information about the coherent patches of the real interface. The small mismatch of the Ag-MgO interface was eliminated by adapting the lattice parameters of both Ag and MgO to 4.20 Å. The relaxation of the Ag atoms with respect to the MgO was carried out in slab geometry with free surfaces on both sides of the interface and periodic boundary conditions. The Brillouin zone of the Ag-MgO was sampled by $1\times4\times8$ k points (spacing of $0.04059\times0.04860\times0.04209$ 1/Å). The model of the polar Ag-MgO interface is depicted in Fig. 2. On both sides of the interface a vacuum of width 5.42 Å was included. The periodic slab geometry of (4|3,2) (Ag|O,Mg) layers for the oxygen-terminated interface and (4|2,3) (Ag|O,Mg) for the magnesium-terminated interface in the *ABCABcabc* stacking sequence was applied to keep the computation manageable. The forces on all ions were relaxed to <0.02 eV/Å using the Broyden-Fletcher-Goldfarb-Shanno[21–24] procedure.

The interface separation after the relaxation of the Ag block across the {111} Ag-MgO interface was 1.55 Å for the oxygen-terminated interface and 2.20 Å for the magnesium-terminated interface. The interplanar spacing between Ag layers in the bulk was 2.19 Å. The free surface of the MgO side of the interface has an O or Mg layer (Fig. 2) as required to keep global stoichiometric MgO. We distinguish here the concept of stoichiometry as applied to surfaces and to whole slabs. Thus we refer to a slab as globally stoichiometric if it contains equal numbers of Mg and O atoms, whereas a surface is stoichiometric if it has no surface excess of Mg or O. For a MgO (111) surface to be stoichiometric it is necessary to remove half of the terminating plane

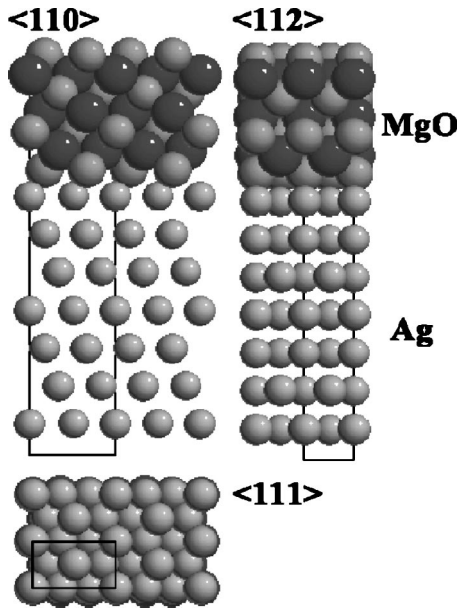

FIG. 3. Schematic illustration of the {111} Ag-MgO model interface.

of Mg or O. The stoichiometric surface would also be charge neutral if the ions carried their formal charges. Nonstoichiometric surfaces of ionic materials are sometimes referred to as "polar" surfaces. For more details see Ref. 25. During the calculation the dimensions of the supercell 23.55 Å $\times$5.144 Å$\times$2.97 Å and 24.97 Å$\times$5.144 Å$\times$2.97 Å for the oxygen and Mg-terminated interfaces were kept fixed. Comparison of calculated polar {222} MgO-Cu interfaces with a slab geometry of (3,3|3) (Mg,O|Cu) layers in the *ABCabc* stacking sequence and (5,5|5) (Mg,O|Cu) yielded similar results.[26] Subsequently, the relaxed Ag coordinates with respect to MgO were used as an input for the relaxation of a larger polar Ag-MgO model, keeping the coordinates of Mg and O unchanged. Figure 3 shows the periodic slab geometry of (7|4,3) (Ag|O,Mg) layers in the *CABCABCabcabca* stacking sequence without the presence of a vacuum.

In principle, the calculation holds for a multilayer. To extract the charge transfer across the interface and the electron redistribution due to metal-oxide bonding the charge-density difference must be calculated. This was performed with CASTEP in the following way: First, the charge density of the Ag-MgO interface was calculated. Afterwards the individual slab calculation of MgO and Ag was carried out in the same supercell by just removing for each case the block of Ag atoms or of MgO, respectively. In all calculations, the number of *k* points and cutoff energy were kept constant. The calculated charge density of the Ag-MgO interface was subtracted from sum of the charge densities of the Ag and MgO slabs to obtain the charge density difference $\Delta\rho(\vec{r})$, which represents the charge redistribution due to the bonding across Ag-MgO. The charge density $\Delta\rho(\vec{r})$ including the bonding environment in the bulk was calculated using DACAPO by subtracting the charge density from the fully self-consistent calculation from the density given by the initial superimposed charge densities of the individual atoms in the ground state. Then, $\Delta\rho(\vec{r})$ includes besides the electron charge transfer and electron redistribution at the interface the ionicity and bonding in the bulk on both sides of the interface.

III. *AB INITIO* HRTEM IMAGE SIMULATION

The charge density calculated with the method described in Sec. II includes a spurious component in the core regions of the atoms, due to the use of pseudopotentials. However, since we are concerned with charge-density differences and their effect on HRTEM simulations, the fixed core part of the density is of no interest. The calculation of the projected potential used for multislice HRTEM image simulations is connected with the charge density via the twofold integration of the Poisson equation in reciprocal space. The implementation of the charge-density difference $\Delta\rho(\vec{r})$ is performed as a correction term for the projected potential. This relation is described as

$$V(\vec{k}) = \frac{2me}{4\pi^2\varepsilon_0 h^2}\left\{\sum_{n,j}\left[\frac{\rho_{n,j}e^{2\pi i\vec{k}\cdot\vec{r}}d\vec{r}}{k^2}\right] - \sum_{nx,ny,nz}\left[\frac{\int\Delta\rho(nx,ny,nz)e^{2\pi i\vec{k}\cdot\vec{r}}d\vec{r}}{k^2}\right]\right\}, \quad (1)$$

which demonstrates the splitting of the charge density into two parts for the calculation of the projected potential $V(\vec{k})$. The charge density $\rho_{n,j}$ denotes the charge of nucleus *j* including the electrons of the neutral atom on site *n* represented by the electron scattering factors as described by Doyle and Turner[6] and the second term represents the correction term $\Delta\rho(\vec{r})$. The charge-density difference $\Delta\rho(\vec{r})$ is integrated over the CASTEP or DACAPO grid *nx*, *ny*, *nz* of the supercell. The charge density difference $\Delta\rho(\vec{r})$ was implemented as a correction term in the source code of the EMS software package.[27] Note that in all HRTEM image simulations the Debye-Waller factor and absorption coefficient were set equal to zero.

The Fourier transformations automatically adapt the CASTEP or DACAPO grid to the EMS grid. This method avoids the need of interpolation of the charge density onto the EMS grid,[9] but the accuracy is limited by the spatial frequency up to which the charge-density calculations were carried out. Nevertheless, the current approach accounts for nonspherical components and redistribution of the charge density. Atomic form factors, which assume rotational symmetry of the charge density of atoms, are thus not applied in the present approach.

IV. COMPARISON BETWEEN *AB INITIO* AND STANDARD HRTEM SIMULATION

We shall refer to image simulations based on first-principles calculations of the charge density as *ab initio* simulations. These can now be compared with the image contrast provided by a standard HRTEM simulation program, e.g., EMS with Doyle and Turner neutral atom scattering factors. In all cases, the EMS program[27] was used to simulate

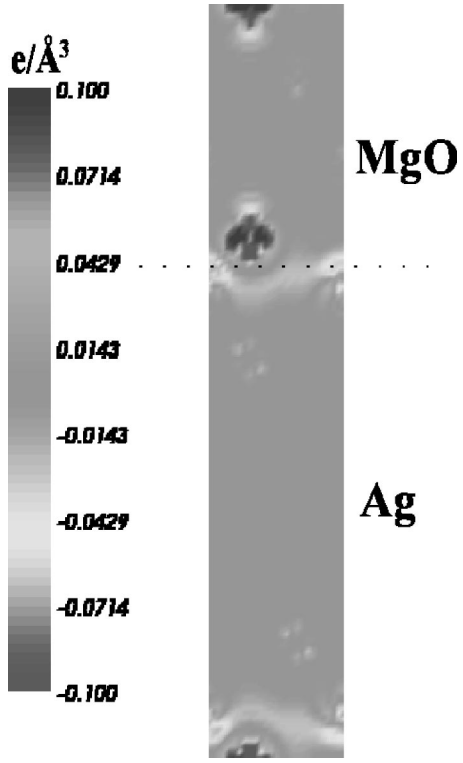

FIG. 4. Charge-density difference $\Delta\rho(\vec{r})=\rho_{\text{Ag-MgO}}(\vec{r})-[\rho_{\text{Ag slab}}(\vec{r})+\rho_{\text{MgO slab}}(\vec{r})]$ of the Ag-MgO interface (CASTEP) referred to self-consistent free surfaces. The cross section of the contour plot goes through (0.5,0,0) to get a cross section of a Ag-O bond at the interface. The range $\pm 0.1\ e/\text{Å}^3$ is chosen for a better visualization. The actual $\Delta\rho$ values range from -1.026 to $0.453\ e/\text{Å}^3$.

the HRTEM images. The input parameters for the simulated images correspond to the ones of the JEOL 4000EX/II in Groningen, operating at 400 kV with an information limit of 1.4 Å (spherical aberration coefficient, 0.97 ± 0.02 mm; defocus spread, 7.8 ± 1.4 nm; beam convergence half-angle, 0.8 mrad).

The *ab initio* HRTEM simulations of bulk MgO and sapphire included the ionic character of the bonding into the projected potentials $V(\vec{k})$ by augmenting the atomic charge densities with the self-consistent charge-density differences. Inversion of the contrast of MgO in the $\langle 110\rangle$ projection can be observed at the thickness (defocus) value of 71 Å (−750 Å) between the conventional simulation and the image simulation corrected with the charge-density map. The convergent beam electron diffraction technique (CBED) and DFT calculation suggested previously that the charge density in MgO could be described as a superposition of spherical Mg^{2+} and O^{2-} ions,[28] although we note that the numerical values of ionic charge are not uniquely defined, and indeed the O^{2-} ion is unstable in vacuum. This high degree of ionicity is presumably responsible for the reversal in contrast in the HRTEM image simulation. By comparison, the incorporation of the ionic environment in sapphire does not significantly change the simulated image based on neutral atoms,[9] a result we reproduced.

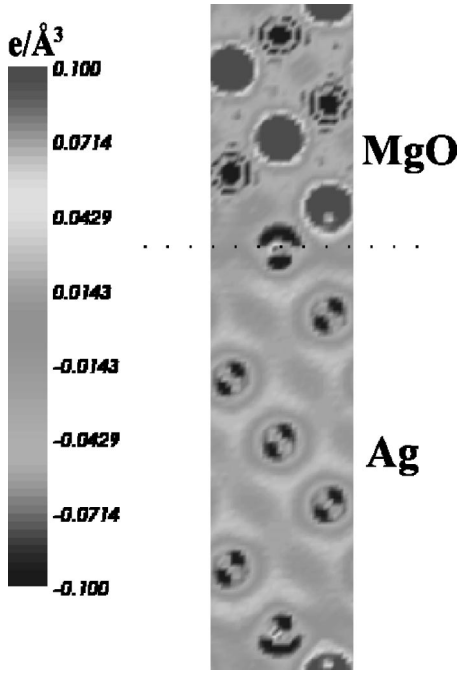

FIG. 5. Charge-density difference $\Delta\rho(\vec{r})=\rho_{\text{Ag—MgO}}(\vec{r})-[\rho_{\text{Ag neutral}}(\vec{r})+\rho_{\text{MgO neutral}}(\vec{r})]$ of the Ag—MgO interface (DACAPO) referred to neutral atoms. The cross section of the contour plot goes through (0.5,0,0) to get a cross section of a Ag-O bond at the interface. The range $\pm 0.1\ e/\text{Å}^3$ is chosen for a better visualization. The actual $\Delta\rho$ values range from -0.243 to $0.393\ e/\text{Å}^3$.

A. {111} Ag—MgO interface (O-terminated)

In the following, three different approaches to the image simulation for {111} Ag-MgO interfaces will be evaluated:

(a) Standard HRTEM simulation using the Doyle-Turner scattering factor.

(b) Standard HRTEM simulation adding a correction term for the charge transfer and charge redistribution only at the interface (CASTEP), i.e., referred to self-consistent free surfaces.

(c) Standard HRTEM simulation adding a correction term for case (b) and the ionicity in MgO (DACAPO), i.e., the charge redistribution is referred to neutral atoms.

Contour plots of the charge-density difference [through (0.5,0,0) to get a cross section of a Ag—O bond] reveal a similar behavior of the charge redistribution at the interface, but as expected not for the bulk phases (see Figs. 4 and 5). Figure 5 shows discontinuities near the core but actually this discontinuity is not real. A plot range of $\pm 0.1\ e/\text{Å}^3$ is chosen for better visualization of the charge density at the interface. The higher electron densities $>0.1\ e/\text{Å}^3$ are not depicted in the contour plots, but were included in the HRTEM correction terms. Furthermore, since we are working with slabs, one would not expect perfect fcc symmetry in the difference charge density at Ag but that we do not see much evidence of any violation of fcc symmetries to graphical accuracy at the central Ag atoms in the cross section shown.

From the contour plots it is hardly possible to conclude about the character of bonding, e.g., if net charge transfer occurs. Calculation of the layer-projected densities of states

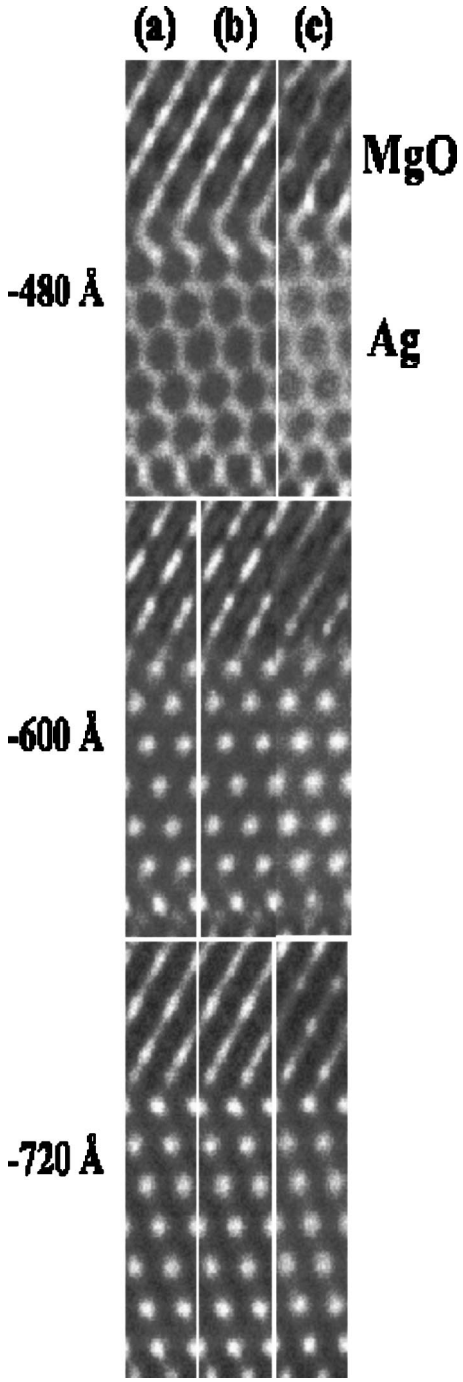

FIG. 6. HRTEM image simulation of Ag-MgO in the ⟨110⟩ viewing direction using defocus values −480, −600, and −720 Å and a thickness of 74 Å.

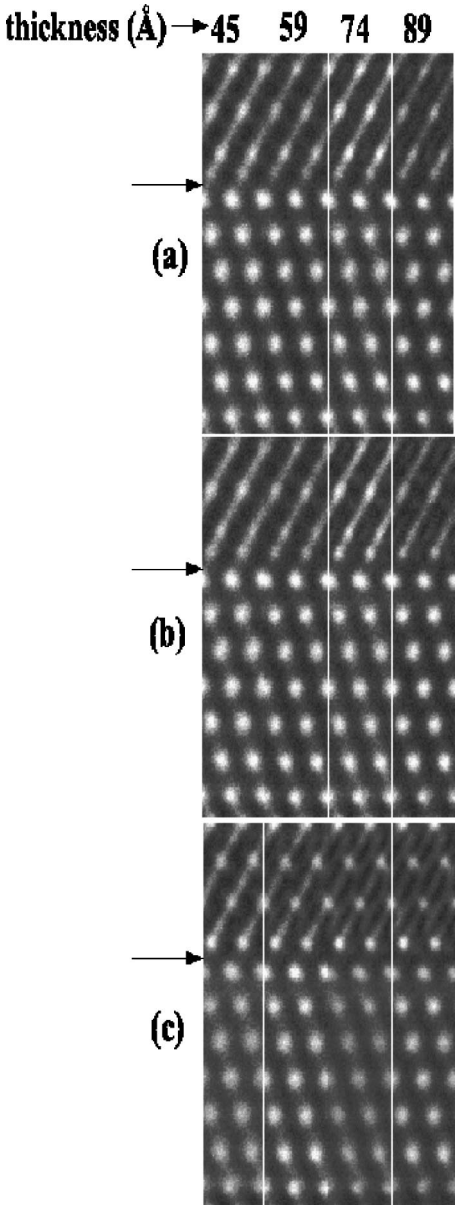

FIG. 7. HRTEM image simulation of Ag-MgO in the ⟨110⟩ viewing direction using a defocus value of −750Å and thicknesses of 45, 59, 74, and 84 Å.

reveals the occurrence of states in the band gap of MgO whose intensity decays exponentially with increasing distance from the metal-oxide interface.[29] These are known as metal-induced gap states (MIGS). MIGS at the MgO side of the interface reduce the electron charge redistribution and charge transfer, due to the less ionic character of the interface. An additional effect of the MIGS is the reduction of the electrostatic potential shift. In contrast, considerable electronegativity would indicate an ionic type of interface, but a calculated layer-by-layer charge transfer, with respect to the self-consistent free surfaces, determined with Mulliken charge population analysis does not exceed 0.18 e/atom, which is in agreement with the polar Cu-MgO interface.[26] The Mulliken charge analysis is used simply to give a qualitative comparison. It is generally recognized that measures of charge transfer are arbitrary, and any method such as Mulliken analysis is best used to describe trends, since the actual numbers will depend on the arbitrary basis set onto which the charge is projected. The MIGS at the oxide side should be a general feature of any metal-oxide interface, as mentioned in Ref. 2.

A set of HRTEM simulated images of the {111} Ag—MgO interface is shown in Figs. 6 and 7. The arrows in Figs. 6 and 7 indicate the interface between the terminating oxygen and silver layer. Figure 6 shows HRTEM simulations

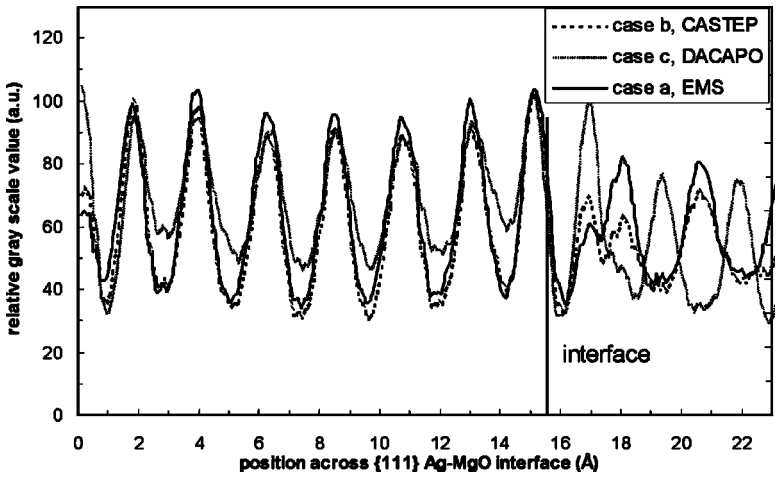

FIG. 8. Line profiles of simulated images across {111} Ag-MgO interface (O-terminated) using a defocus value of −750 Å and a thickness of 74 Å. These line profiles correspond to the simulated images in the third through fourth of Fig. 7.

for three different defocus values of −480, −600, and −720 Å for cases (a), (b), and (c) with a constant thickness of 74 Å. Figure 6(a) refers to the standard simulation with the Doyle-Turner scattering factor without any correction term. The scattering factors are used to describe neutral and spherical atoms. In Fig. 6(b) the standard simulation corrected with the charge-density difference obtained with CASTEP (see Sec. II). The subtraction of the charge density of the interface with the individual slabs of Ag and MgO (by just removing in the first calculation MgO and second case Ag) was performed with a constant supercell dimension and cuttoff energy. This means that the corrected HRTEM image in Fig. 6(b) includes no bonding environment and ionic character of the bulk, but the charge transfer and charge redistribution directly at the interface. In Fig. 6(c) the standard simulation is corrected with the charge density obtained with DACAPO (see Sec. II). This correction term includes the calculated correction term in Fig. 6(b) and additionally the bonding environment in the bulk. This was performed by subtracting the fully self-consistent calculation from the density given from the initial charge of the individual atoms in the ground state. The simulated HRTEM in Fig. 6(c) is corrected with the charge density including the bonding environment and the charge redistribution at the interface. The terminating oxygen monolayer changes contrast among the three different cases; note especially that a difference exists between the contrast of the standard HRTEM simulation [case Fig. 6(a)] and the corrected HRTEM simulation [see case Fig. 6(c)] for a given defocus value. Including the bonding of individual atoms in the correction term [case (c)] the brightness is increased at the terminating oxygen monolayer compared with the brightness of the oxygen layers in the bulk (see Fig. 7, right column). For all defocus-thickness variations a contrast change in the corrected HRTEM simulations in the outmost Ag layer at the Ag-MgO interface is barely detectable. The electrons on the metal side at the interface may screen any perturbation and inhibit a contrast change at the metal side of the interface.

Line profiles of simulated images across the {111} Ag-MgO interface (O-terminated) using defocus value of −750 Å and a thickness of 74 Å are depicted in Fig. 8. The line profiles correspond to the simulated images in the third row of Fig. 7. The line profile of the corrected image simulation of case (c) shows that the contrast minima and maxima are inverted compared with simulation of neutral MgO [case (a) and (b)], whereas in the bulk of Ag similar contrast behavior is observed in all cases (see Fig. 8). Furthermore, the terminating oxygen layer (when compared to the other

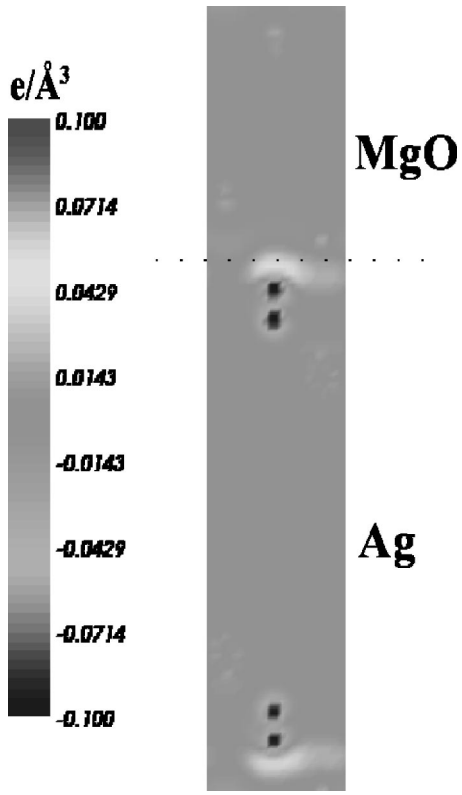

FIG. 9. Charge-density difference $\Delta\rho(\vec{r}) = \rho_{\mathrm{Ag—MgO}}(\vec{r}) - [\rho_{\mathrm{Ag\ slab}}(\vec{r}) + \rho_{\mathrm{MgO\ slab}}(\vec{r})]$ of the Ag-MgO interface. The cross section of the contour plot goes through (0.5,0,0) to get a cross section of an Ag-Mg bond at the interface. The range $\pm 0.1\ e/\text{Å}^3$ is chosen for a better visualization. The actual $\Delta\rho$ values range from -0.1473 to $0.0425\ e/\text{Å}^3$.

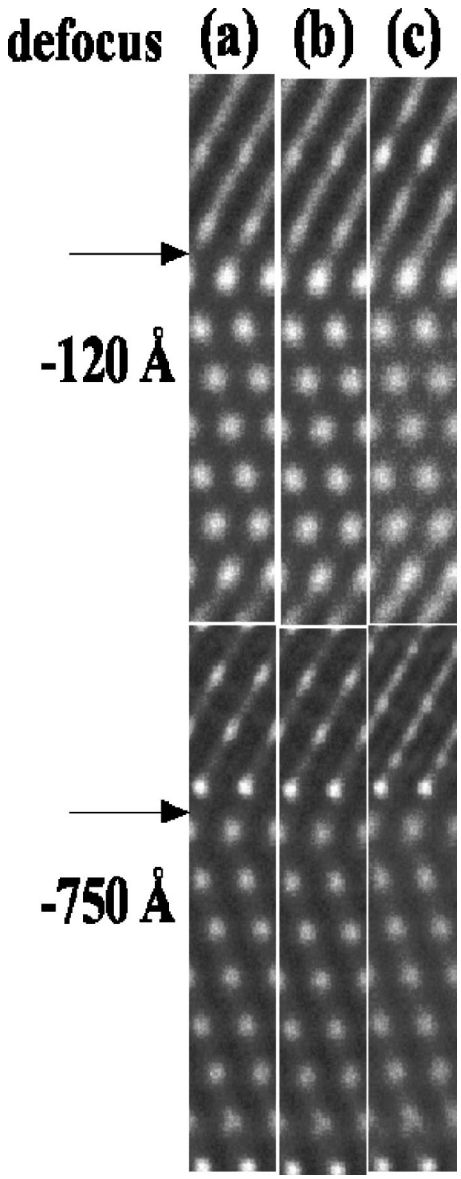

FIG. 10. HRTEM image simulation of a Mg-terminated Ag-MgO interface in the ⟨110⟩ viewing direction using defocus values −120 Å and −750 Å with a thickness of 74 Å. The panels (a), (b), and (c) correspond to the defined correction terms, as described in Sec. IV.

oxygen layers in the bulk) has a much higher intensity (is much brighter) for case (c) than for case (a). This effect is similar to what is experimentally observed in Fig. 1. There it was earlier assumed to be an increased brightness on the terminating Ag layer. According to the present calculations the first oxygen layer should particularly have a deviating contrast. There is a large difference between CASTEP and DECAPO, although each theory is taking into account the electron transfer. The origin of this difference lies in the fact that two different definitions of electron transport are being considered, based on either neutral atoms as the starting point or on free slabs of the Ag and MgO, so the use of CASTEP or DECAPO, in this context is of secondary importance.

B. {111} Ag-MgO interface (Mg-terminated)

The same procedure was applied to the Mg-terminated {111} Ag-MgO interface. A contour plot of the charge density difference through (0.5,0,0) to get a cross section of an Ag-Mg bond for case (b) (including only the charge redistribution at the interface) is displayed in Fig. 9. Figure 9 indicates that the charge redistribution in the terminating Ag layer is less pronounced at the Mg-terminated layer than in the case of an oxygen-terminated interface (Fig. 4). A set of HRTEM simulated images is shown in Fig. 10 of an Mg-terminated {111} Ag—MgO interface. The arrows in Fig. 10 indicate the interface between the terminating magnesium and silver layer.

The line profile of the corrected image simulation of case (c) shows that the contrast minima and maxima are inverted compared with a simulation excluding the bonding environment of the bulk MgO [case (a) and (b)], whereas in the bulk of Ag similar contrast behavior is observed in all cases, as shown in Fig. 11. At the terminating Ag and Mg layers, the contrast does not change significantly (compare within Figs. 10 and 11). This is in agreement with the small charge redistribution present at the Mg-terminated {111} Ag—MgO interface compared with the corresponding O-terminated interface (compare Fig. 4 versus Fig. 9).

V. DISCUSSION AND CONCLUSIONS

In the DFT plane-wave calculations, we have used the LDA approximation (CASTEP code) as well as the GGA approximation (DACAPO code), in accordance with the generated ultrasoft pseudopotentials used in both codes. Indeed we have not analyzed the GGA versus LDA treatments of exchange and correlation to see which gives better results. To do so would require a theory that is superior to both of them, or sufficiently accurate experimental data. Unfortunately neither is currently available to us. We must be content at this point to say that the two approaches give qualitatively similar results. As stated before, for reasons of consistency we used the same exchange-correlation functional for the applications as was used to generate the component pseudopotentials. Nevertheless, the point is that we need to work with two different pseudopotentials, one generated with LDA, the other with GGA, and this was achieved by using the two different codes. This is purely a matter of convenience, and no scientific issues seem to be at stake: both are plane-wave pseudopotential codes, so given the same pseudopotentials and the same exchange-correlation functional, they should give identical results. Perhaps in an ideal world we would have used the same basic code with modular implementations of both GGA and LDA.

Furthermore it should be stressed that in previous experimental work[1] we concentrated on the dislocation network along semicoherent interfaces. Our reason for not considering the triangular network of dislocations, or any other network of dislocations, is simply that we want to make image simulations explicitly of the coherent patches between misfit dislocations, for comparison of the electron density models with each other and with experimental data taken from such coherent patches. It would be difficult to make image simu-

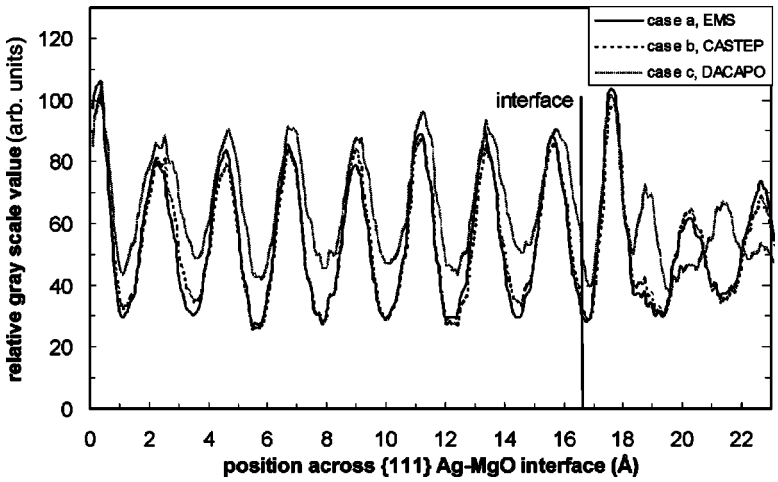

FIG. 11. Line profiles of simulated images across {111} Ag-MgO interface (Mg terminated) using defocus value of −750 Å and a thickness of 74 Å. These line profiles correspond to the simulated images in the right column of Fig. 10.

lations of the complete semicoherent interface, i.e., including the misfit dislocations, because the periodicity of the supercell, and hence the number of atoms required, would be very large with only a 3% misfit—about 25 times larger than with the 15% misfit.[1]

The MIGS diminish the ionic character of metal-oxide bonding, resulting in less charge transfer and electrostatic potential shift at the interface. From the observed change in contrast between conventional and *ab initio* HRTEM image simulations it can be concluded that not only the ionicity and nonspherical atomic form factors in the slabs of pure oxide, but also the charge transfer between oxide and metal is important. Some effort is necessary to calculate *ab initio* charge-density difference maps, but this is recovered by an increase in the reliability of quantitative image matching. In particular, the reliance on conventional HRTEM image simulations of oxides can lead to a misinterpretation of the experimental image. For instance, the estimated thickness obtained with image matching of the experimental image reveals that the calculated image is thinner using screened potentials (incorporating the ionicity in HRTEM image simulations) than when using the neutral atom potential.[30] Any HRTEM image simulation starts with the determination of atomic scattering factors to calculate the projected potential. It should be pointed out that the scattering factors from Doyle and Turner,[5] parametrized as the sum of four Gaussians, are only valid up to 2.0 nm^{-1}. This leads to an underestimate of the scattering greater than 2.0 nm^{-1}, but a 400-kV high-resolution microscope with a resolution of 0.16 nm resolves scattering angles to about 10 mrad (2.0 nm^{-1} is equivalent to 33 mrad at 400 kV). On the other hand, the calculated atomic scattering factors from Rez *et al.*[31] are quite similar to those of Doyle and Turner.[6] Thus, we assume that the atomic scattering factors themselves are not a source of error.

In conclusion, the ionicity of oxides and the charge redistribution in oxides and at interfaces play a significant role and should be incorporated in HRTEM image simulations. Self-consistent charge-density calculations were used to generate a correction term to take these effects into account.

It has been mentioned that for a defocus of −750 Å a reversal of the contrast of bulk MgO in the ⟨110⟩ projection occurs due to this correction. On the other hand, it seems that the ionicity is not important for sapphire in HRTEM image simulations.[9] This was verified in the present work. It contradicts the findings of Stobbs and Stobbs[7] where the ionicity in sapphire seems to be important for HRTEM image simulations. The chosen high defocus value of −750 Å in most of the HRTEM image simulations (Figs. 7–10) reflects the maximum difference between the conventional HRTEM image simulation (Doyle and Turner scattering factors[6]) and the corrected HRTEM image simulation using first-principles calculations of the charge density redistribution. *Ab initio* HRTEM image simulations on polar {111} Ag-MgO interfaces reveal significant differences in contrast compared with conventional image simulations.

At oxygen-terminated {111} Ag-MgO the bonding between metal and oxide is responsible for the difference in brightness at the interface comparing conventional and *ab initio* HRTEM image simulations. In contrast, the magnesium-terminated {111} Ag-MgO interface shows no contrast change between conventional and *ab initio* HRTEM image simulations. The enhanced contrast compared with the contrast in the bulk structure at the interface originates from the position of the Ag atoms at the interface rather than from bonding changes across the Ag-MgO interface. We include calculations for both the O-terminated and Mg-terminate interfaces. Although it has been shown previously[32] that the Mg-terminated interface is less favorable to adhesion than the oxygen-terminated interface, we would not rule out its existence under all conditions, for example if the ratio of Mg to O activities were higher. From an experimental viewpoint is should be realized that both terminations are feasible, depending on the partial pressure of oxygen.[33,34]

ACKNOWLEDGMENTS

The work is part of the research program of the Foundation of Fundamental Research on Matter (FOM-Utrecht) and has been made possible by financial support form the Netherlands Organization for Research (NWO-The Hague) and the Netherlands Institute for Metals Research. We are grateful to Dr. Alexander Lozovoi for fruitful discussions and the help with the calculations in the Atomistic Simulation Group at Queen's University Belfast.

*Author to whom correspondence should be addressed. Email address: hossonj@phys.rug.nl

[1] J. Th. M. De Hosson and B. J. Kooi, in *Handbook of Surfaces and Interfaces in Materials*, edited by H. S. Nalwa, (Academic Press, New York, 2001), Vol. 1, Chap. 1.
[2] M. Finnis, J. Phys.: Condens. Matter **8**, 5811 (1996).
[3] A. G. Evans, M. F. Ashby, and J. P. Hirth in *Metal-Ceramic Interfaces*, edited by M. Rühle (Pergamon, Oxford, 1990).
[4] D. Hofmann and F. Ernst, Ultramicroscopy **53**, 205 (1994).
[5] G. Möbus and M. Rühle, Philos. Mag. A **56**, 54 (1994).
[6] P. A. Doyle and P. S. Turner, Acta Crystallogr., Sect. A: Cryst. Phys., Diffr., Theor. Gen. Crystallogr. **24**, 390 (1967).
[7] S. H. Stobbs and W. M. Stobbs Inst. Phys. Conf. Ser. **147**, 83 (1995).
[8] G. Möbus, G. Gemming, T. Nüchter, W. Exner, M. Gumbsch, P. Weickenmeier, A. Wilson, and M. Rühle, in *Proceedings of the 55th Annual Meeting of MSA*, Cleveland, pp. 1159–1160 (1997).
[9] T. Gemming, F. Ernst G. Möbus, M. Exner, and M. Rühle, J. Microsc. **190**, 89 (1998).
[10] D. R. Rasmussen and C. B. Carter, Ultramicroscopy **32**, 337 (1990).
[11] R. E. Dunin-Borkowski, Ultramicroscopy **83**, 193 (2000).
[12] W. Mader and B. Maier, J. Phys.: Condens. Matter **1**, 867 (1990).
[13] B. J. Kooi, H. B. Groen, and J. Th. M. de Hosson, Acta Mater. **45**, 3587 (1997).
[14] H. B. Groen Ph.D. thesis (University of Groningen, 1999).
[15] M. C. Payne, M. P. Teter, D. C. Allan, T. A. Arias, and J. D. Joannopoulos, Rev. Mod. Phys. **64**, 1045 (1992).
[16] B. Hammer, L. Hansen, and J. K. Nørskov, Phys. Rev. B **59**, 7413 (1999).
[17] D. Vanderbilt, Phys. Rev. B **41**, 7892 (1990).
[18] J. Perdew and A. Zunger, Phys. Rev. B **23**, 5048 (1981).
[19] J. Perdew, J. A. Chevary, S. H. Vosko, K. A. Jackson, M. R. Pederson, D. J. Singh, and C. Fiolhais, Phys. Rev. B **46**, 6671 (1992).
[20] M. Fuchs, M. Bockstedte, E. Pehlke, and M. Scheffler, Phys. Rev. B **57**, 2134 (1998).
[21] C. G. Broyden, J. Inst. Math. Appl. **6**, 222 (1970).
[22] R. Fletcher, Comput. J. **13**, 317 (1970).
[23] D. Goldfarb, Math. Comput. **24**, 23–26, 1970.
[24] D. F. Shanno, Math. Comput. **24**, 647 (1970).
[25] M. W. Finnis, Phys. Status Solidi **166**, 397 (1998).
[26] R. Benedek, D. N. Seidman, M. Minkoff, L. H. Yang, and A. Alavi, Phys. Rev. B **60**, 16 094 (1999).
[27] P. A. Stadelmann, Ultramicroscopy **21**, 131 (1987).
[28] J. M. Zuo, M. O. O'Keeffe, P. Rez, and J. C. H. Spence, Phys. Rev. Lett. **78**, 4777 (1997).
[29] D. A. Muller, D. A. Shashkov, R. Benedek, L. H. Yank, J. Silcox, and D. N. Seidman, Phys. Rev. Lett. **80**, 4741 (1998).
[30] K. Hiratsuka, Philos. Mag. B **63**, 1087 (1991).
[31] D. Rez, P. Rez, and I. Grant, Acta Crystallogr., Sect. A: Found. Crystallogr. **50**, 481 (1994).
[32] R. Benedek, M. Minkoff, and L. H. Yang, Phys. Rev. B **54**, 7697 (1996).
[33] M. Backhaus-Ricoult, Acta Mater. **48**, 4365 (2000).
[34] M. Backhaus-Ricoult and S. Laurent, Mater. Sci. Forum **294–296**, 173 (1999).